



Synthesis, Characterization, Cyclic Voltammetric and Biological Studies of 2-Hydroxy-2-Methyl Propiophenone Sulfaguanidine Azomethine ligand and its Mononuclear Cu(II) Complex

ISHWAR CHAND BALAAE, NARESH KUMAR VERMA, MONIKA JHARWAL,
SALONI MEENA and SARITA VARSHNEY*

Department of Chemistry, University of Rajasthan, Jaipur, 302004, Rajasthan, India.

*Corresponding author E-mail: icsurela@gmail.com

<http://dx.doi.org/10.13005/ojc/380212>

(Received: December 27, 2021; Accepted: March 15, 2022)

ABSTRACT

A new Cu(II) complex with Schiff base ligand 2-hydroxy-2-methyl propiophenone sulfaguanidine (HMPHG) has been prepared in alcoholic medium and investigated by elemental analysis and spectroscopic methods. The ligand and its Cu(II) complex were subjected to cyclic voltammetric studies using glassy carbon electrode with variable scan rate at various pH levels. The electrochemical studies show single Irreversible reduction wave for ligand while quasi-reversible wave for its Cu(II) complex. For comparative studies, electrochemical measurements were carried out in different polarity solvents. Various kinetic variables such as charge transfer coefficient (α_n), diffusion coefficient ($D_o^{1/2}$) rate constant ($K_{i,h}^0$) were also determined from cyclic voltammograms measurement. Further, ligand and its Cu(II) complex were analyzed for antimicrobial studies.

Keywords: 2-Hydroxy-2-methylpropiophenone, Sulfaguanidine, Cyclic voltammetry, Charge transfer coefficient (α_n), Diffusion coefficient ($D_o^{1/2}$), Rate constant ($K_{i,h}^0$) and Antimicrobial study.

INTRODUCTION

Schiff bases are derived from condensation of a primary amine with an active carbonyl compound under acidic basic medium or with heat¹⁻². These are the compounds with azomethine group and studied first by Hugo Schiff in 1864. A number of curative compounds have been obtained from Schiff base reactions which are being used for medicine and pharmaceutical purposes due to their versatile biological importance such as anti-

inflammatory drugs³⁻⁴ antimicrobial⁵⁻⁷ antispasmodic⁸ tuberculosis⁹ anticancer¹⁰, antioxidant¹¹ and anthelmintic properties¹². Schiff bases are also used as catalyst,¹³⁻¹⁴ dyes and pigments, polymer¹⁵⁻¹⁶ and corrosion inhibitors¹⁷⁻¹⁸. The Schiff base ligands played an important role in the development of coordination chemistry and were involved as essence in the improvement of bioinorganic chemistry and optical materials¹⁹. Many important sulfa drugs are known as preventive and therapeutic compounds against several bacterial infections due to $-SO_2NH-$



moiety. Schiff bases derived from sulfa drugs have been synthesized and used as ligand to prepare a potent metal complex.²⁰⁻²¹ The cyclic voltammetric technique is important electrochemical technique which provides information regarding reduction and oxidation potential, formation of intermediates and most importantly the information concerning reversibility of electron transfer across the electrode solution interface, which helps in elucidating kinetics and mechanism of reaction taking place at the electrode. In this paper we are reporting synthesis, spectral analysis and cyclic voltammetric studies of HMPSG and its Cu(II) complex.

EXPERIMENTAL

Synthesis of Schiff base ligand-Analytical grade chemicals employed in present study. The Schiff base ligand HMPSG was prepared by adding a hot methanolic solution of 2-hydroxy-2-methylpropiophenone to a hot methanolic solution of sulfaguandine with fast stirring in equimolar ratio. The reaction mixture refluxed for 5-6 h at 60°C. The condensation product separated on cooling, was filtered off, washed several time and purified by repeated recrystallization from ethanol solvent, anhydrous calcium chloride was used for drying the compound (Figure 1).

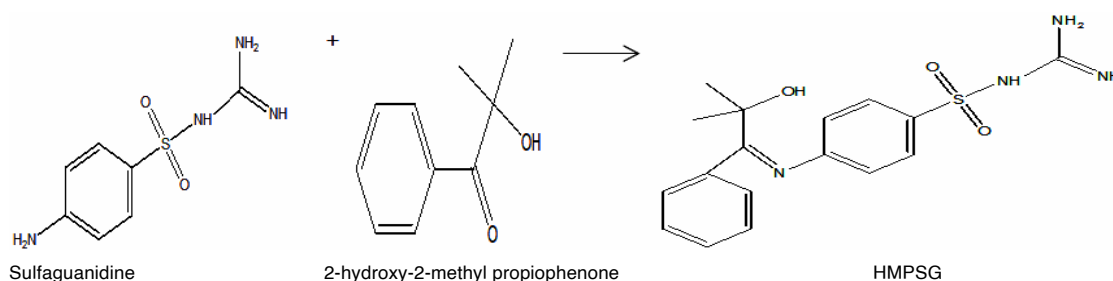


Fig. 1. Scheme of HMPSG Schiff base ligand preparation

Synthesis of copper(II) complex

Copper(II) complex of HMPSG were prepared by adding a methanolic solution of $(\text{CH}_3\text{COO})_2\text{Cu}\cdot\text{H}_2\text{O}$ with vigorous stirring to HMPSG methanolic solution in ratio of 1:2. The obtained mixture was heated under reflux with stirring for 4 h at 60°C and then allowed to evaporate into its one third volumes and cooled. The obtained deep green coloured complex was separated and washed with methanol and dried in vacuum over anhydrous calcium chloride (yield 68%).

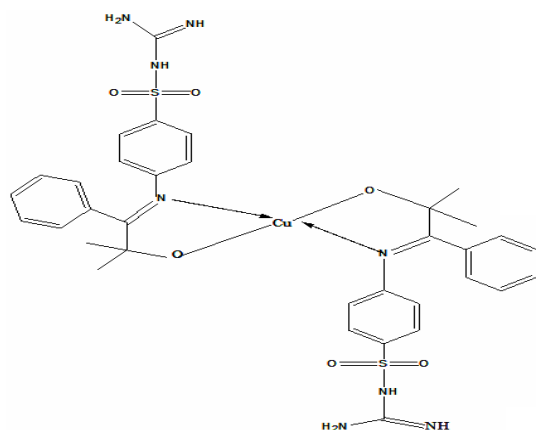


Fig. 2. Copper(II) Complex of HMPSG ligand

RESULTS AND DISCUSSION

Micro analytical technique was used

for elemental analysis on C,H,N,S,O elemental analyzer. Melting point apparatus was used for recording melting point and found 182°C for HMPSG and 205°C for Cu(II) complex.

Infrared spectral studies

The IR studies of the prepared ligand and Cu(II) complex were obtained in the range 4000-440 cm^{-1} . Absence of absorption bands for amino group of sulfaguandine phenyl ring and the ketonic group of 2-hydroxy-2-methylpropiophenone in spectra of ligand are characteristic which indicate the condensation between carbonyl group and $-\text{NH}_2$ group. A new peak at 1625 cm^{-1} is characteristic $\nu_{(\text{C}=\text{N})}$ of azomethine group confirmed above the same. A band of $\nu_{(\text{C}=\text{N})}$ in the region 1614-1620 cm^{-1} in spectra of the complexes show the shift of the band to lower wave number which indicate the coordination of ligands with metal through nitrogen atom. Absence of a broad band in the region 3300-3450 cm^{-1} for $-\text{OH}$ group in complex indicates the de-protonation of OH proton before coordination. On comparing the SO_2 , SO_2-NH , $\text{C}=\text{NH}$, $=\text{C}-\text{NH}_2$ bands in the complex confirmed that they are not associate in coordination. The appearance of the new peak in the region 445-465 cm^{-1} and 510-560 cm^{-1} assignable to $\nu_{(\text{Cu}-\text{O})}$ and $\nu_{(\text{Cu}-\text{N})}$ respectively consider the bonding of copper ion to O and N atoms.

Table 1: Elemental analyses

S no.	Composition of ligand/complex (M.Wt.)	colour	Yield (%)	Elemental analysis(%): found(cal.)					
				C	H	N	O	S	Cu
1	C ₁₇ H ₂₀ N ₄ O ₃ S -360.432	Pale yellow	76	56.58	5.75	15.56	13.48	8.6	
				-56.64	-5.59	-15.54	-13.31	-8.89	
2	C ₃₄ H ₃₈ CuN ₈ O ₆ S ₂ -780.321	Deep green	68	52.19	4.9	14.32	12.27	8.2	8.14
				-52.17	-4.92	-14.31	-12.31	-8.19	(8.12)

Cyclic voltammetric studies of HMPHG Schiff base ligand

The cyclic voltammetric data were recorded with fully computer controlled electro analytical system, using three electrode cell assembly with glassy carbon as working electrode. The cyclic voltammograms of above introduced ligand were recorded between +800mV to -1500mV in the scan rate interval of 50-250 mV/sec, at constant pH and concentration of experimental solution. The electrochemical behavior of HMPHG was recorded in acetones, methanol and DMF solvents, using phosphate buffer and BR buffer of different pH values. The cyclic voltammetric data for ligand are summarized in Table 2-5 and Fig. 3-6 showed the cyclic voltammograms of HMPHG in DMF-phosphate buffer, acetone phosphate buffer, methanol phosphate buffer and methanol BR buffer. The Fig. 3 shows the cyclic voltammograms that was recorded at pH 7.0 in DMF-phosphate buffer for HMPHG ligand. The peak potential value shifted from -950mV to -1030mV at 50-250 mVs⁻¹ scan rates and peak current (μA) values increases from 29.40 μA to 36.30 μA with same scan rates indicating that the electrode process is irreversible. Fig. 4 represent potential current curves at a scan rate 50-250 mVs⁻¹ in acetone-phosphate buffer at PH 5.0, 7.0, 8.2 (Fig. 4A,B,C respectively). The obtained cyclic voltammograms show one irreversible cathodic peak at all scan rate

and at all taken pH medium. The peak potential value swept from -890mV to -975mV in aforementioned pH medium. Peak current value rises from 10.5μA to 49.5 μA with same pH. Cyclic voltammograms of 1mM HMPHG in CH₃OH-phosphate buffer at PH 5.0, 7.0, 8.2 are shown in Fig. 5 (A, B and C) respectively. For comparative studies of HMPHG ligand in methanol-phosphate buffer, potential was applied in the range of +700mV to -1600mV. All CV curves shows that E_{pc} value shifted to more negative cathodic direction and I_{pc} value also increases with acidic to basic media at 50-250 mV/s scan rates (Table 3). The Fig. 6 shows the current potential curves of HMPHG in CH₃OH-BR buffer at 50,100,150,200 and 250 mVs⁻¹ scan rate at PH 5.0, 7.0, 8.2. The shape of the reduction wave in all cyclic voltammograms of HMPHG shows the irreversible nature of electrode process. Thus kinetic variables such as charge transfer coefficient (α_n), diffusion coefficient (D_o^{1/2}) rate constant (K_{f,h}^o) have been calculated using following equations²²⁻²⁵ and detailed in Table 2-5.

$$|E_p - E_{p2}| = \frac{1.857RT}{\alpha_n F} = \left(\frac{47.7}{\alpha_n}\right) mV \quad (1)$$

$$I_p = 3.01 \times 10^5 n(\alpha_n)^{1/2} ACD_0^{1/2} v^{1/2} \quad (2)$$

$$E_p = \frac{RT}{\alpha_n F} \left[0.78 + \ln\left(\frac{D_0}{k_{f,h}}\right) + \ln\left(\frac{\alpha_n F v}{RT}\right)^{1/2} \right] \quad (3)$$

Table 2: Scan rate V/s voltammetric variables (1mM HMPHG ligand in acetone-phosphate Buffer at different pH i.e. 5, 7, 8.2) (Fure. 4)

pH	v (mVs ⁻¹)	E _{pc} (mV)	I _{pc} (μA)	E _{p/2} (mV)	I _{pc} /v ^{1/2}	α _n	D _o ^{1/2} (cm ² s ⁻¹)	k _{f,h} ^o (cm.s ⁻¹)
5	50	-890	10.5	-790	1.484924	0.477000	6.766939	9.40E-10
	100	-900	11.4	-792	1.140000	0.441667	5.398893	2.92E-09
	150	-910	13.1	-796	1.069611	0.418421	5.204345	6.45E-09
	200	-920	14.9	-820	1.053589	0.477000	4.801305	7.64E-10
	250	-925	16.2	-810	1.024578	0.414783	5.007050	7.12E-09
7	50	-910	14.6	-800	2.064752	0.433636	9.868523	4.19E-09
	100	-922	19.3	-824	1.930000	0.486735	8.706795	6.72E-10
	150	-933	22.4	-835	1.828952	0.486735	8.250940	6.33E-10
	200	-940	29.3	-847	2.071823	0.512903	9.105045	2.78E-10
	250	-955	35.0	-862	2.213594	0.512903	9.728088	2.46E-10
8.2	50	-920	16.2	-800	2.291026	0.397500	11.43691	1.43E-08
	100	-940	27.4	-830	2.740000	0.433636	13.09589	4.74E-09
	150	-952	32.1	-850	2.620954	0.467647	12.06278	1.28E-09
	200	-963	41.1	-872	2.906209	0.524176	12.63384	1.62E-10
	250	-975	49.5	-884	3.130655	0.524176	13.60955	1.52E-10

Table 3: Scan rate V/s voltammetric variables (1mM HMPSG ligand in methanol-phosphate buffer at different pH (5, 7, 8.2) (Figure 5)

pH	v(mVs ⁻¹)	E _{pc} (mV)	I _{pc} (μA)	E _{p/2} (mV)	I _{pc} /v ^{1/2}	α _n	D _o ^{1/2} (cm ² s ⁻¹)	k ^o _{th} (cm.s ⁻¹)
5	50	-900	11.4	-790	1.612203	0.433636	7.705559	3.87E-09
	100	-915	15.9	-805	1.590000	0.433636	7.599438	4.19E-09
	150	-929	18.5	-813	1.510519	0.411207	7.413838	8.67E-09
	200	-940	23.3	-825	1.647559	0.414783	8.051519	8.03E-09
	250	-949	28.5	-836	1.802498	0.422124	8.731765	6.48E-09
7	50	-920	18.6	-810	2.630437	0.433636	12.57223	4.51E-09
	100	-940	25.1	-810	2.510000	0.366923	13.04168	4.99E-08
	150	-954	32.1	-836	2.620954	0.404237	12.97443	1.31E-08
	200	-973	36.8	-848	2.602153	0.3816000	13.25793	2.62E-08
	250	-980	42.7	-857	2.700585	0.387805	13.64892	2.16E-08
8.2	50	-930	19.1	-830	2.701148	0.477000	12.30938	8.13E-10
	100	-952	27.7	-848	2.770000	0.458654	12.87314	1.55E-09
	150	-965	35.9	-865	2.931223	0.477000	13.35786	7.98E-10
	200	-978	39.6	-876	2.800143	0.467647	12.88749	9.87E-10
	250	-989	43.4	-884	2.744857	0.454286	12.81747	1.48E-09

Table 4: Scan rate V/s voltammetric variables (1mM HMPSG ligand in methanol-BR Buffer at different pH (5, 7, 8.2) (Figure 6)

pH	v(mVs ⁻¹)	E _{pc} (mV)	I _{pc} (μA)	E _{p/2} (mV)	I _{pc} /v ^{1/2}	α _n	D _o ^{1/2} (cm ² s ⁻¹)	k ^o _{th} (cm.s ⁻¹)
5	50	-942	20.4	-835	2.884996	0.445794	13.59957	2.18E-09
	100	-956	25.4	-850	2.540000	0.45000	11.91721	1.82E-09
	150	-967	31.3	-870	2.555634	0.491753	11.47024	3.85E-10
	200	-974	33.9	-872	2.397092	0.467647	11.03247	9.09E-10
	250	-983	34.5	-879	2.181972	0.458654	10.14037	1.11E-09
7	50	-950	29.4	-843	4.157788	0.445794	19.59937	2.74E-09
	100	-965	31.3	-860	3.130000	0.454286	14.61595	1.63E-09
	150	-978	34.3	-882	2.800583	0.496875	12.50467	2.81E-10
	200	-985	36.3	-888	2.566798	0.491753	11.52034	3.16E-10
	250	-998	37.2	-902	2.352735	0.496875	10.50501	2.07E-10
8.2	50	-964	35.2	-869	4.978032	0.502105	22.11095	3.11E-10
	100	-982	43.1	-875	4.310000	0.445794	20.31689	2.30E-09
	150	-997	41.3	-880	3.372131	0.407692	16.62208	7.47E-09
	200	-1012	44.4	-916	3.139554	0.496875	14.01818	1.88E-10
	250	-1020	46.3	-935	2.928269	0.561176	12.30293	1.31E-11

Table 5: Scan rate V/S voltammetric variables (1mM 2-hydroxy-2methyl propiophenone in various solvents like acetone, methanol DMF in phosphate Buffer at pH 7

solvent	v(mVs ⁻¹)	E _{pc} (mV)	I _{pc} (μA)	E _{p/2} (mV)	I _{pc} /v ^{1/2}	α _n	D _o ^{1/2} (cm ² s ⁻¹)	k ^o _{th} (cm.s ⁻¹)
Acetone	50	-910	14.6	-800	2.064752	0.433636	9.868523	4.19E-09
	100	-922	19.3	-824	1.930000	0.486735	8.706795	6.72E-10
	150	-933	22.4	-835	1.828952	0.486735	8.250940	6.33E-10
	200	-940	29.3	-847	2.071823	0.512903	9.105045	2.78E-10
	250	-955	35	-862	2.213594	0.512903	9.728088	2.46E-10
Methanol	50	-920	18.6	-810	2.630437	0.433636	12.57223	4.51E-09
	100	-940	25.1	-810	2.510000	0.366923	13.04168	4.99E-08
	150	-954	32.1	-836	2.620954	0.404237	12.97443	1.31E-08
	200	-973	36.8	-848	2.602153	0.3816000	13.25793	2.62E-08
	250	-980	42.7	-857	2.700585	0.387805	13.64892	2.16E-08
DMF	50	-950	29.40	-843	4.157700	0.445700	39.20290	4.36E-09
	100	-973	31.3	-860	3.130000	0.422124	15.16253	4.80E-09
	150	-994	34.3	-882	2.800583	0.425893	13.50658	3.22E-09
	200	-1020	37.60	-890	2.658700	0.454200	24.83280	1.48E-09
	250	-1030	36.30	-918	2.295800	0.425800	22.14680	3.75E-09

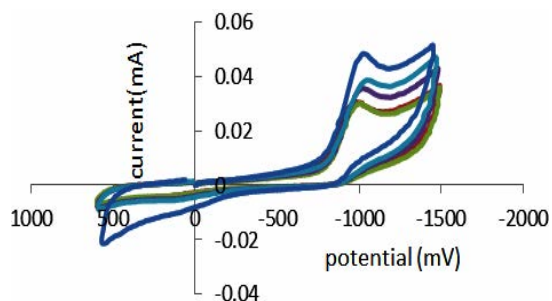
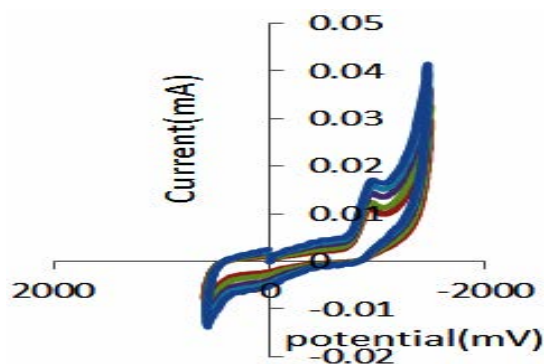
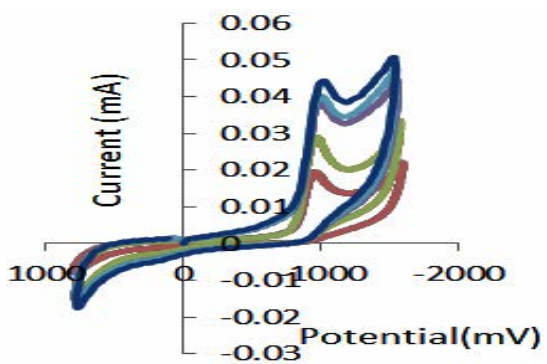


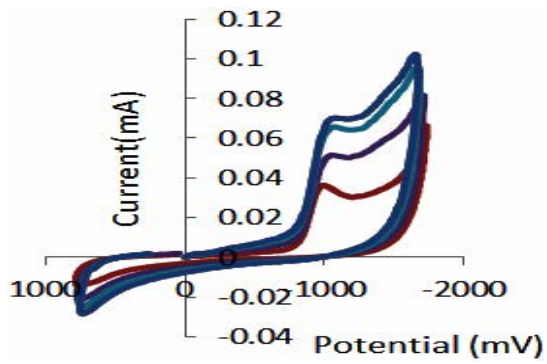
Fig. 3. Cyclic voltammograms of 1mM HMPSG in DMF-phosphate buffer at 7.0 pH



(A)

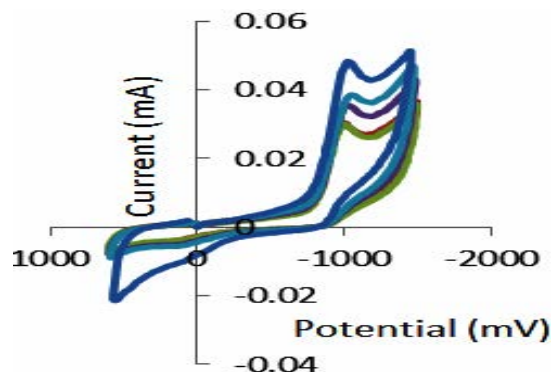


(B)

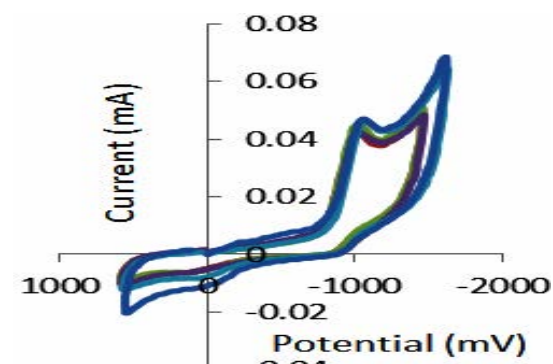


(C)

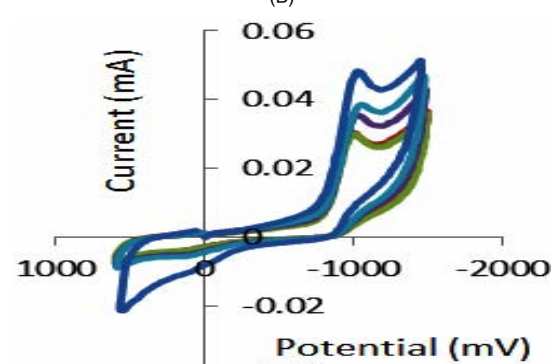
Fig. 4. Cyclic voltammograms of 1mM HMPSG in acetone-phosphate buffer at PH 5.0, 7.0, 8.2 showed in Fig. A, B and C respectively



(A)



(B)



(C)

Fig. 5. Cyclic voltammograms of 1mM HMPSG in CH_3OH -phosphate buffer PH 5.0, 7.0, 8.2 showed in Fig. A, B and C respectively

Effect of change of scan rate

The impact of scan rate upon reduction of ligand was investigated from the analysis of cyclic voltammograms. The investigation was obtained by changing the scan rates from 50, 100, 150, 200 and 250 mV/s. The cathodic peak potential shifted to more negative value with increasing scan rate which indicates irreversibility of electrochemical process. The linear relationship between cathodic peak potential (E_{pc}) with $\ln v$ confirmed the irreversibility

of the reduction process (Fig. 7, 8 and 9). In all the cyclic voltammograms the current function ($I_{pc}/v^{1/2}$) has been found to be fairly constant with respect to scan rate (Fig. 10) showing that the electrode process is diffusion controlled²⁶⁻²⁷.

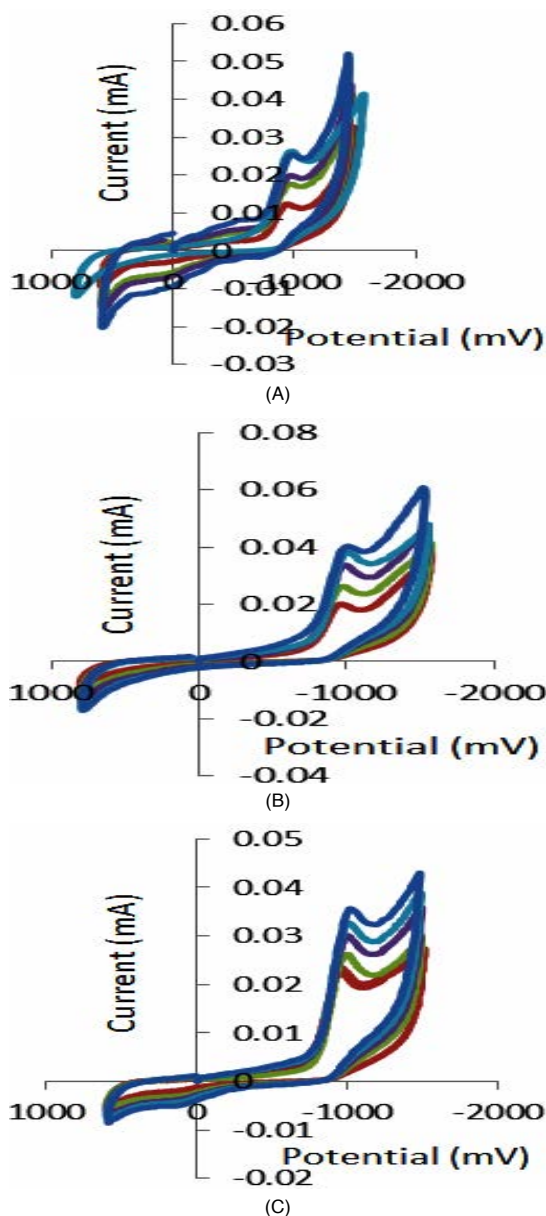


Fig. 6. Cyclic voltammograms of 1mM HMPSG in CH_3OH -BR buffer at PH 5.0, 7.0, 8.2 showed in Fig. A, B and C respectively

Effect of solvent

The electrochemical behavior is affected by nature of solvent. Comparative studies have been done to analyze the electrochemical parameters of ligand. Cyclic voltammograms of HMPSG were

recorded in various solvent like acetone, CH_3OH and DMF with phosphate Buffer at pH 7. It showed that the negative peak potential value is maximum in DMF solvent and minimum in acetone solvent. [Table 5]. This trend is similar to the trend in viscosity, dielectric constant and polarity of this solvents²⁸⁻²⁹.

Effect of pH

The pH effect on electrochemical behaviour of ligand was also investigated in the pH range (5, 7 and 8.2) of experimental solution. The peak potential value of ligand is found to be changed with the pH value of the solution and shifting towards more negative value was observed for higher pH. This indicates participation of proton during electrode process. The reduction is easier at low pH in comparison of higher pH. It confirmed the formation of easily reducible protonated intermediate during the reduction (Table 1, 2, 3).

Effect of buffer

To observe the effect of buffer medium electrochemical behavior of HMPSG ligand were recorded in phosphate buffer and Britton-Robinson buffer (BR) with methanol solvent at 50-250 mVs sweep rate and at different pH (5, 7, 8.2) (Fig. 6). These cyclic voltammograms show that cathodic peak potential sweeps towards high negative value in BR buffer solution compared to phosphate buffer solution at same scan rate and pH values indicates that the polarity of buffer solution affected electrochemical behaviour of redox species. The reduction potential value in methanol-phosphate buffer is reported to vary from -900mV to -989 mV at 50 to 250 mVs^{-1} scan rates at different pH. While in methanol -BR buffer, E_{pc} values varies from -942mV to 1020 mV at 50-250 mVs^{-1} , suggesting that reduction process is more convenience in high polarity phosphate buffer solution.³⁰

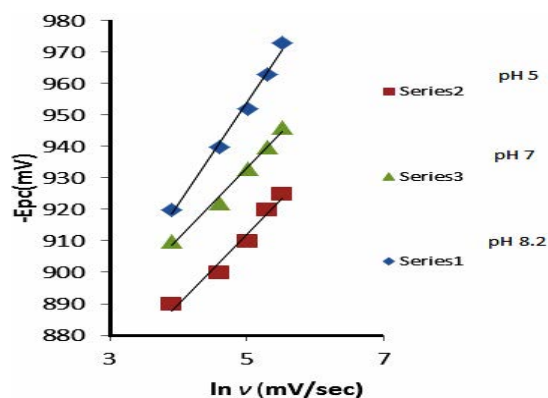


Fig. 7. Reduction potential V/S $\ln v$ for 1mM HMPSG in acetone-phosphate buffer

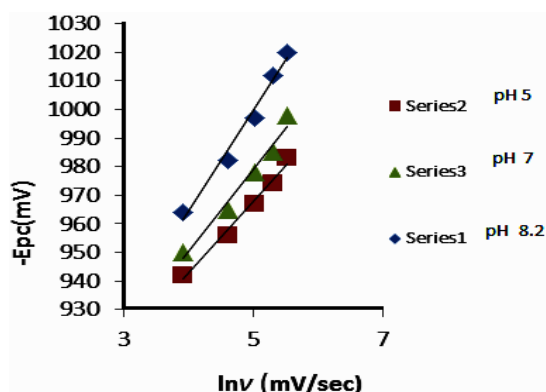


Fig. 8. Reduction potential V/S $\ln v$ for 1 mM HMPSG in CH_3OH -BR buffer

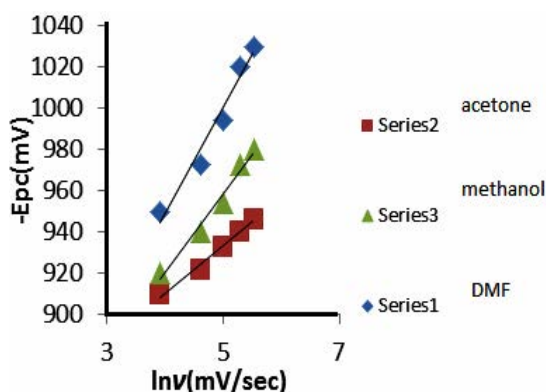


Fig. 9. Reduction potential V/S $\ln v$ for 1 mM HMPSG in different solvents in phosphate Buffer at pH 7

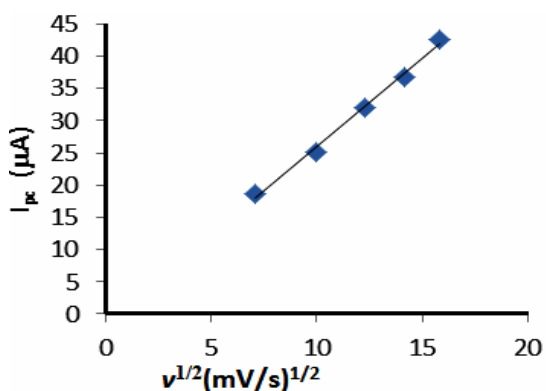


Fig.10. I_{pc} vs $v^{1/2}$ for 1mM HMPSG in methanol-phosphate buffer at pH 7

Cyclic voltammetric studies of Copper(II) complex of HMPSG

The electrochemical behaviour of Cu(II) complex has been investigated by cyclic voltammetric technique in DMF solvent containing NaClO_4 as supporting electrolyte with different scan rates varying from 100 to 300 mVs^{-1} . The cyclic voltammograms show the negative potential of complex ranging from -0.51V to -0.54V, and in reverse scan a corresponding anodic wave occurs in the range of -0.18V to -0.17V and the peak separation (ΔE_p) varies from 0.326V to 0.377 V. The ligand does not show cathodic and anodic potential as in the above range, so the redox process is assigned to the copper centre only. The CV of complex shows a quasi-reversible peak corresponding to the formation of Cu(II)/Cu(I) couple at given potential. The peak separation (ΔE_p) varying from 0.326V to 0.377 V and the ratio between the anodic and cathodic peak current is less than unity ($I_{pa}/I_{pc} < 1$) corresponding to a simple one electron transfer process³¹⁻³³. A linear dependence between cathodic peak current (I_{pc}) and the square of the scan rates ($v^{1/2}$) have been also observed (Fig.12). This fact implies that these electrochemical process are mainly diffusion controlled.

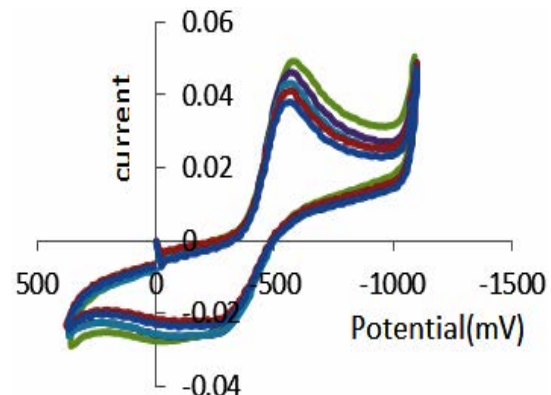


Fig. 11. Collective scan on the voltammograms of 1mM Cu(II) complex of HMPSG in DMF- NaClO_4

Table 6: Effect of scan rate on voltammetric variables of 1 mM Cu(II) Complex of HMPSG in DMF- NaClO_4 solvent (Figure 11)

v mVs^{-1}	E_{pc} (mV)	$E_{p,a}$ (mV)	ΔE_p (mV)	$E^{1/2}$ (mV)	I_{pc} (μA)	$I_{p,a}$ (μA)	$I_{p,a}/I_{p,c}$	$I_{p,c}/v^{1/2}$
100	-515	-189	326	-442	25.9	15.2	0.586873	2.59
150	-520	-185	335	-448	31.8	17.8	0.559748	2.596459
200	-532	-182	350	-454	35.8	18.1	0.505587	2.531442
250	-540	-175	365	-460	41.9	24.9	0.594272	2.649989
300	-547	-170	377	-467	46.7	25.6	0.54818	2.696226

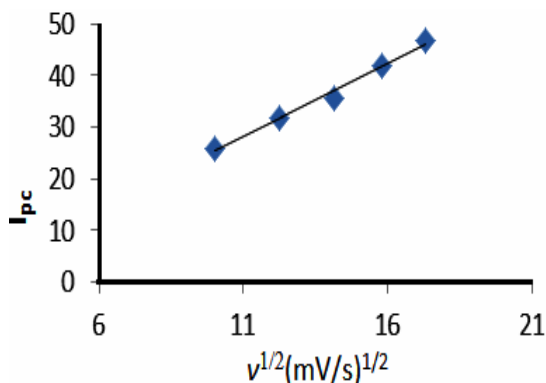


Fig. 12. I_{pc} VS $v^{1/2}$ for 1 mM Cu(II) complex of HMPSG

Biological studies of HMPSG ligand and its Cu(II) complex

The synthesized ligand and its Cu(II)

complex have been subjected to antimicrobial analysis. *Gram-positive* (*Staphylococcus aureus*) and *Gram-negative* bacteria (*Escherichia coli*) and fungi *Aspergillus niger*, *Candida albicans* were selected to study the antimicrobial activity. Ciprofloxacin and Ketoconazole were used as the standard for bacterial and fungal studies respectively. Well diffusion method is used. The results are incorporated in tables 7 & 8. The microbial activity of compound was determined on the basis of inhibited zone size around each well. The results reveal that there is considerable increase in toxicity of the complex as compared to the ligand. Complex is found to be more active against all organisms used than the ligand. It can be explained by Tweedy's Chelation theory.³⁴⁻³⁶

Table 7: Antibacterial studies of schiff base ligand HMPSG and its Cu(II) complex

Anti-bacterial	<i>Staphylococcus aureus</i>				<i>Escherichia coli</i>			
	HMPSG		Cu(II) complex		HMPSG		Cu(II) complex	
Stock Conc. $\mu\text{g/mL}$	Zone of Inhibition (mm)	Activity index	Zone of Inhibition (mm)	Activity index	Zone of Inhibition (mm)	Activity index	Zone of Inhibition (mm)	Activity index
20	13	0.541	14	0.583	14	0.583	14	0.583
30	14	0.583	15	0.625	16	0.666	17	0.708
40	15	0.625	16	0.666	21	0.875	20	0.833
50	19	0.791	20	0.833	22	0.916	24	1.000
60	21	0.875	22	0.916	26	1.083	28	1.166

Table 8: Antifungal studies of Schiff base ligand HMPSG and its Cu(II) complex

Anti-fungal	<i>Aspergillus niger</i>				<i>Candida albicans</i>			
	HMPSG		Cu(II) complex		HMPSG		Cu(II) complex	
Stock Conc. $\mu\text{g/ml}$	Zone of Inhibition (mm)	Activity index	Zone of Inhibition (mm)	Activity index	Zone of Inhibition (mm)	Activity index	Zone of Inhibition (mm)	Activity index
20	10	0.666	10	0.666	11	0.733	12	0.800
30	12	0.800	13	0.866	13	0.866	14	0.933
40	13	0.866	14	0.933	14	0.933	16	1.066
50	15	1.000	17	1.133	17	1.133	18	1.200
60	17	1.133	19	1.266	20	1.333	23	1.533

CONCLUSION

In this research paper, the complex of Cu(II) with schiff base ligand prepared from 2-hydroxy-2-methyl propiophenone and sulfaguandine was synthesized and characterized by spectral techniques. Cyclic voltammetric studies of the ligand confirmed that the electrochemical behaviour of HMPSG ligand is irreversible and diffusion controlled under the various pH scale and sweep

rate range from 50 mV/s to 250 mV/s. It was found that the value of reduction potential depends on scan rate, pH of experimental solution and different buffer medium. The E_{pc} and $E_{p_{1/2}}$ swept to more cathodic value with increasing pH and scan rate. The cyclic voltammograms of Cu(II) complex displayed a quasireversible one electron transfer redox process. The antimicrobial effects of prepared compounds were investigated on different type's bacteria and fungi.

ACKNOWLEDGMENT

Authors express their sincere thanks to the Department of Chemistry, University of Rajasthan,

Jaipur for providing research facilities. The authors Naresh Kumar Verma, Monika Jharwal are thankful to CSIR, New Delhi and Saloni Meena is thankful to UGC, New Delhi for financial assistance.

REFERENCES

1. Abu-Khadra, A.; Farag, R.; Abdel-Hady, A. *Am. J. Analyt. Chem.*, **2016**, *7*, 233-245.
2. Rauf, A.; Shah, A.; Khan, A. A.; Shah, A. H.; Abbasi, R.; Qureshi, I. Z.; Ali, S. *Spectrochim. Acta, Part A.*, **2017**, *176*, 155-167.
3. Shukla, S.; Mishra, A.P. *Arab. J. Chem.*, **2019**, *12*(7), 1715-1721.
4. Murtaza, S.; Akhtar, M.S.; Kanwal, F.; Abbas, A.; Ashiq, A.; Shamim, S. *J. Saudi Chem. Soc.*, **2017**, *21*, S359-S372.
5. Anaconda, J.; Pineda, Y.; Bravo, A.; *Camus, J. Med. Chem. (Los Angeles)*, **2016**, *6*, 467-4736.
6. Hossain, B. D.; Camellia, M. K.; Ud din, N.; Zahan, K.; Banu, L. A.; Haque, M. *Asian J. Chem. Sci.*, **2019**, *6*(1), 1-8.
7. Charles, A.; Sivaraj, K. *Res. J. Life Sci. Bioinform. Pharm. Chem. Sci.*, **2019**, *5*(2), 984.
8. Chaubey, A. K.; Pandeya, S. N. *Int. J. Pharmtech Res.*, **2012**, *4*, 590-598.
9. Cordelia, U.; Dueke, E.; Tolulope, M.; Fasinaa, A. E.; Oluwalanaa, O. B.; Familoni, A.; Jack, M.; Mphalele, B.; Onubuoguca, C. *Sci. Afr.*, **2020**, *9*, e00522.
10. Tadele, K.T.; Tsega, T.W. *Anti-Cancer Agents Med. Chem.*, **2019**, *19*(15), 217-219.
11. Kalaiarasi, G.; Dharani, S.; Puschmann, H.; Prabhakaran, R. *Inorg. Chem. Commun.*, **2018**, *97*, 34-38.
12. Maddireddy, M.; Kulkarni, A.D.; Bagihalli, G.B.; Malladi, S. *Helv. Chim. Acta.*, **2016**, *99*, 562-572.
13. Adam, M. S. S.; Al Omair, M. A.; Ullah, F. *Res. Chem. Intermed.*, **2019**, *45*, 4653-4675.
14. Adam, M. S. S.; El-Hady, O. M.; Ullah, F. R. *Soc. Chem.*, **2019**, *9*, 34311.
15. González, D. M.; Cisterna, J.; Brito, I.; Roisnel, T.; Jean-Hamon, J.; Manzur, C. *Polyhedron.*, **2019**, *162*, 91-99.
16. JieLai, F.; LingChiu, L.; LingLee, L.; YiLu, W.; Yi-ChunLai.; Shangwu Ding.; Ying Chen, H.; Kuo-Hui, W. *Polymer.*, **2019**, *182*, 121812.
17. Hassan, M. A.; Heakal, B. H.; Younis, A.; Bedair, M. A.; Elbialy, Z. I.; Abdelsalam, M. M. *Egypt. J. Chem.*, **2019**, *62*(9), 1603-1624.
18. Das, M.; Biswas, A.; Kund, B.K.; Charmier, M. A.J.; Mukherjee, A.; Mobin, S.M.; Udayabhanu, G.; Mukhopadhyay, S. *Chem. Eng. J.*, **2019**, *357*, 447-457.
19. Arroudj, S.; Bouchouit, M.; Bouchouit, K.; Bouraiou, A.; Messaadia, L.; Kulyk, B.; Figa, V.; Bouacida, S.; Sofiani, Z.; Taboukhat, S. *Opt. Mater.*, **2016**, *56*, 116-120.
20. Mondal, S.; Mandal, S. M.; Mondal, T. K.; Sinha, C. *J. Mol. Struct.*, **2017**, *1127*, 557-567.
21. Rani, S.; Sumrta, S.H.; Chohan, Z.H. *Russ. J. Gen. Chem.*, **2017**, *87*(8), 1834-1842.
22. Sharma, P.; Kumar, A.; Sharma, M. *Indian J. Chem.*, **2006**, *45A*, 872.
23. Bard, A.J.; Faulkner, L.R.; Leddy, J.; Zoski, C.G. Wiley New York., **1980**, *2*.
24. Meena, L.; Choudhary, P.; Varshney A.K.; Varshney, S. *Port. Electrochim. Acta.*, **2019**, *37*, 271-283.
25. Noel, M.; Vasu, K.I. Aspect Publication, London., **1990**.
26. Abdallah, M.; Alharbi, A.; Morad, M.; Hameed, A.M.; Al-Juaid, S.S.; Foad, N.; Mabrouk, E.M. *Int. J. Electrochem. Sci.*, **2020**, *15*, 6522-6548.
27. Aoki, K.J.; Taniguchi, S.; Chen, J. *J. Am. Chem. Soc.*, **2020**, *5*, 29447-29452.
28. Kumawat, G. L.; Choudhary, P.; Varshney, A.; Varshney, S. *Orient. J. Chem.*, **2019**, *35*(3), 1117-1124.
29. Davood, A.; Yoonesi, B.; Soleymanpour, A. *Int. J. Electrochem. Sci.*, **2010**, *5*, 459-477.
30. Choudhary, P.; Kumawat, G.L.; Sharma R.; Varshney, S. *Int. J. Pharm. Sci. & Res.*, **2018**, *9*(11), 4601-09.
31. Andrew, F.P.; Ajibade, P.A. *Int. J. Electrochem. Sci.*, **2021**, *16*, 150950.
32. Shaju, K. S.; Joby, T. K.; Raphael, V.P.; Nimmy Kuriakose, S. *J. Appl. Chem.*, **2014**, *7*(10), 64-68.
33. Losada, J.; Del Peso, I.; Beyer, L.; *Inorg. Chim. Acta.*, **2001**, *321*, 107-115.
34. Dharmaraj, N.; Viswanathamurthi, P.; Natarajan, K. *Transition Met. Chem.*, **2001**, *26*, 105-109.
35. Hassan, F.S.M.; Mahmoud Fayez M.; Abdalla, N. *Open J. Inorg. Non met. Mater.*, **2020**, *10*, 15-29.
36. Wanale, S.G.; Pachling, S.P. *Res. J. Pharm. Biol. Chem. Sci.*, **2012**, *3*(2), 64.